Astrophysics of Magnetically Collimated Jets Generated from Laser-Produced Plasmas

A. Ciardi,[1] T. Vinci,[2] J. Fuchs,[2] B. Albertazzi,[2,3] C. Riconda,[4] H. Pépin,[3] and O. Portugall[5]

[1]*LERMA, Observatoire de Paris, Université Pierre et Marie Curie, École Normale Superieure, UMR 8112 CNRS, 5 Place Jules Jannsen, 92195 Meudon, France*

[2]*LULI, CNRS, École Polytechnique, Université Pierre et Marie Curie, CEA, 91128 Palaiseau, France*

[3]*INRS-EMT, Varennes, Québec J3X 1S2, Canada*

[4]*LULI, Université Pierre et Marie Curie, École Polytechnique, CNRS, CEA, 75252 Paris, France*

[5]*Laboratoire National des Champs Magnétiques Intenses, 31400 Toulouse, France*

(Received 8 October 2012; published 9 January 2013)

The generation of astrophysically relevant jets, from magnetically collimated, laser-produced plasmas, is investigated through three-dimensional, magnetohydrodynamic simulations. We show that for laser intensities $I \sim 10^{12}$–$10^{14}\,\mathrm{W\,cm^{-2}}$, a magnetic field in excess of ~0.1 MG, can collimate the plasma plume into a prolate cavity bounded by a shock envelope with a standing conical shock at its tip, which recollimates the flow into a supermagnetosonic jet beam. This mechanism is equivalent to astrophysical models of hydrodynamic inertial collimation, where an isotropic wind is focused into a jet by a confining circumstellar toruslike envelope. The results suggest an alternative mechanism for a large-scale magnetic field to produce jets from wide-angle winds.

DOI: 10.1103/PhysRevLett.110.025002 PACS numbers: 52.30.Cv, 52.38.−r, 98.38.Fs

The ejection of mass in the form of bipolar jets is ubiquitous in astrophysics, and it is widely recognized to be the result of a large-scale, magnetic field extracting energy from an accreting system [1]. Models of magnetohydrodynamic (MHD) jet launching [2] rely on differential rotation to shear the poloidal magnetic field component, $\mathbf{B}_{\mathrm{pol}} = B_r\hat{\mathbf{r}} + B_z\hat{\mathbf{z}}$, and generate a toroidal component, B_θ, which is necessary to power and collimate the flow. The magnetic structure then consists of helical field lines, with the collimation of the outflow determined by the component of the Lorentz force perpendicular to $\mathbf{B}_{\mathrm{pol}}$, namely $F_\perp = -\frac{B_\theta}{\mu_0 r}\nabla_\perp(rB_\theta) + j_\theta B_{\mathrm{pol}}$. The first term of $F_\perp$ is the essence of self-collimation, and its role in jet collimation and stability has been studied not only through multidimensional simulations [3], but also in experiments using dense, magnetized plasmas [4–6]. These experiments can in fact produce flows that are well approximated by the Euler MHD equations, and whose invariant properties allow meaningful scaling of laboratory to astrophysical fluid dynamics [7]. However, in collimation solely by the poloidal magnetic field, the term $F_\perp \sim j_\theta B_{\mathrm{pol}}$, still remains to be clarified. For static plasma columns, the confinement was studied in the context of linear theta pinches [8]. In astrophysics, poloidal collimation can act in the magnetosphere-disc region on scales of a few AU (1 astronomical unit $\sim 1.5 \times 10^{13}$ cm), where the collimation of a stellar wind depends critically on the magnetic field anchored in the disc [9]. On scales of tens of AU, it leads to the formation of axially elongated cavities [10], and may also serve to recollimate potentially unstable MHD jets [11]. On even larger scales, it is an essential component of the collimation of outflows embedded in magnetized envelopes [12].

In this Letter we establish the astrophysical relevance of coupling laser-produced plasmas with a strong magnetic field, as a platform to study jet collimation. Although interest in nonrelativistic jetlike flows has instigated a number of experiments using high-power lasers [13], these so far remain limited to unmagnetized jets [14,15]. For laser intensities in the range 10^{12}–$10^{14}\ \mathrm{W\,cm^{-2}}$, corresponding to laser energies $E_L \sim 5$–500 J, with nominal laser parameters for the pulse duration of $\tau_L = 1$ ns, focal spot diameter of $\phi = 750\ \mu$m, and wavelength of $\lambda = 1.064\ \mu$m, we show that under conditions now accessible to current facilities [16], a long-duration ($t \gg 10$ ns), strong magnetic field (>0.1 MG) can magnetically collimate jetlike flows. The basic configuration studied consists of a solid planar target immersed in an externally applied, homogeneous magnetic field B_0 parallel to the z axis, and perpendicular to the target. Using a combination of two- and three-dimensional (3D) simulations, we provide a theoretical description of the mechanism responsible for generating hydrodynamic jets via a conical shock, from an uncollimated plasma. These results suggest a novel mechanism where wide-angle winds from stars and discs, may be recollimated into *hydrodynamic* jets by a large-scale, poloidal magnetic field.

For a given applied magnetic field and laser energy, a characteristic collimation radius can be estimated from the equilibrium between ram and magnetic pressures ($\rho v^2 \sim B_0^2/8\pi$) as $R_{\mathrm{coll}}(\mathrm{cm}) \sim 0.8[E_K(J)/B_0(T)2]^{1/3}$, where the bulk kinetic energy is parametrized as a fraction f of the laser energy deposited on target, $E_K = fE_L$. Numerically we find $f \sim 0.3$–0.5, which is consistent with experimental measurement [17]; however, considering only the radial expansion, better estimates are obtained for $f \sim 0.1$–0.2.

The related collimation time scale is estimated as $\tau_{\rm coll} \sim R_{\rm coll}/v_{\rm exp}$, where the expansion velocity [18] is $v_{\rm exp}({\rm cm/s}) = 4.6 \times 10^7 I^{1/3}\lambda^{2/3}$ (I is the intensity in units of 10^{14} W cm^{-2} and λ is the laser wavelength in μm). Figure 1 represents $R_{\rm coll}$ and $\tau_{\rm coll}$ as a function of applied magnetic field, and shows that to magnetically collimate a jetlike flow with a radius of a few millimeters, field intensities $\gtrsim 0.1$ MG need to be applied for several tens of nanoseconds.

Numerically, we investigate the interaction of a laser-generated plasma plume from solid foil targets (C, Al, Cu) with an externally applied, steady-state magnetic field in the range $B_0 = 0$–0.4 MG. Although in this regime a strong (MG) magnetic field can be generated from nonparallel gradients of electronic temperature and density [19], it remains localized both in time and space [20,21], and does not affect the plasma dynamics over the time scales ($\gg \tau_L$) and length scales ($\gg \phi$) of interest to our work. The initial plasma evolution is modeled in axisymmetric, cylindrical geometry with the two-dimensional, three-temperature, Lagrangian, radiation hydrodynamic code DUED [22], coupled with SESAME EOS tables [23]. The plasma profiles of density, momentum, and temperature (electronic and ionic) are then (at $t = 1.2$ ns) linearly mapped onto a 3D Cartesian grid with a superimposed uniform magnetic field, and used as the initial condition for the 3D Eulerian, resistive MHD code GORGON [24,25]. We shall see that 3D calculations are necessary to capture the nonaxisymmetric modes of MHD instabilities developing in the flow at late times ($t \gg \tau_L$). Simulations were run at different resolutions ($\Delta x = 35$–65) μm and also with the initial velocity field randomly perturbed ($\delta v/v_0 \sim 0.05$–0.15). The results are quantitatively similar, with only small differences in the azimuthal structure of the flow.

The magnetic collimation of a laser-generated plasma plume may be characterized by three main phases. These are shown in Fig. 2, for a simulation of an aluminium target, with $I = 1.5 \times 10^{14}$ W cm^{-2} and $B_0 = 0.2$ MG. The laser propagation is antiparallel to the z axis, and the target is at $z = 0$ mm. The first phase [Fig. 2(a)] corresponds to the initial expansion of the plasma plume, its deceleration by the radial component of the Lorentz force $F_r = j_\theta B_z$, and the formation of a shell of shocked plasma delineating the boundaries of the plume. The time shown ($t = 5$ ns) corresponds approximately to the maximum radial extent ($R_{\rm coll} \sim 3$–4 mm) reached by the thermally driven expanding plasma. Times are given from the end of the laser pulse, unless otherwise stated. Because of the relatively high temperatures, $T_e \sim 300$–500 eV, the electrical conductivity is high and dissipation of magnetic flux via diffusion is small. This is characterized by a relatively high magnetic Reynolds number, ${\rm Re}_M = 1.4 \times 10^{-20} vL/\eta \sim 100$, where $v \sim 10^7$ cm/s, $L \sim 0.1$ cm and $\eta \sim 1.5 \times 10^{-16}$ s are the characteristic velocity, length scale, and resistivity respectively. Therefore the magnetic field is "frozen" in the plasma, and the field lines are swept laterally by the flow and accumulate in the shock envelope. In addition, the field lines are bent, generating a radial component of the magnetic field which produces an additional axial force ($F_z = j_\theta B_r$). Although this is generally small compared to the thermal pressure gradients, we shall see later that the curvature of the field lines plays an important role on the stability of the flow. Velocities in the plume (few $\times 100$ km/s) are well in excess of the fast magnetoacoustic speed $c_{\rm ma}$, and the deceleration of the plasma produces a fast shock; the magnetoacoustic speed, $c_{\rm ma} = \sqrt{c_A^2 + c_s^2}$, is a combination of the Alfven speed, $c_A = B/\sqrt{4\pi\rho}$, and the adiabatic sound speed, $c_s = \sqrt{\gamma p/\rho}$, with ratio of specific heats $\gamma = 5/3$.

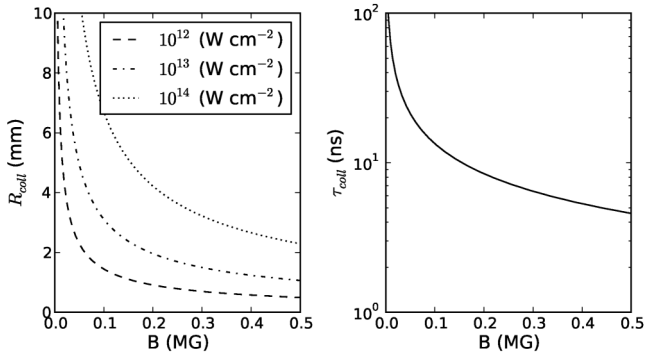

FIG. 1. Initial collimation radius (left) and time scale (right) calculated with $f = 0.1$. Because of the dependence adopted for $v_{\rm exp} \propto I^{1/3}$, the collimation time scale is independent of the laser intensity.

The second phase is the formation of a jet via a standing conical shock. The propagation in the axial direction is essentially unimpeded by the magnetic field, and the cavity becomes more elongated in time. The shock envelope is oblique with respect to the flow velocity, and compresses the component of the magnetic field tangential to the shock, while maintaining the tangential velocity continuous. This axial focusing mechanism is elucidated in Fig. 2(c), where the velocity vectors show the flow being refracted across the shock, sliding along the walls of the cavity, before finally converging towards the axis. Furthermore, as demonstrated by the contour lines of the fast magnetoacoustic Mach number, $M_{\rm ma} = v/c_{\rm ma}$ [Fig. 2(a)], the plasma in the shock envelope remains superfast magnetosonic. Its collision on the axis can then generate either a conical shock, if the reflection is regular, or a Mach reflection [Fig. 2(b)] consisting of an axisymmetric triple shock structure, with two oblique (conical) shocks, and a planar shock (Mach disk) [26]. In either case, further acceleration of the flow and its collimation into a narrow jet occur as the plasma reaching the tip of the cavity is redirected axially by a conical shock. The whole flow configuration described so far shares many important features with astrophysical models of shock focused inertial confinement [27]. In those models the *hydrodynamic*

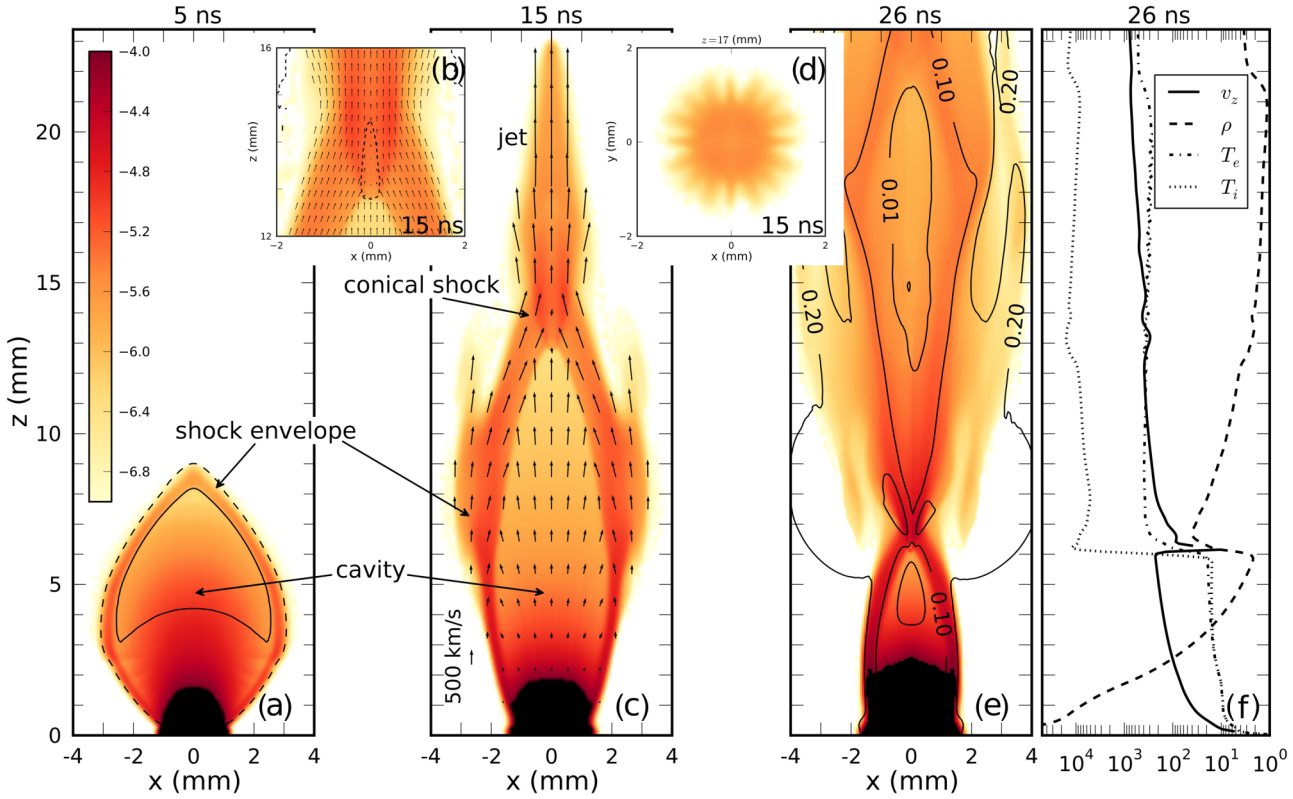

FIG. 2 (color online). Color maps correspond to the logarithmic density in g cm^{-1}. Panels (a), (c), and (e) show a cut through the middle of the computational domain in the xz plane. Contour lines in panel (a) correspond to $M_{\rm ma} = 1$ (dashed) and $M_{\rm ma} = 10$ (solid). Velocity vectors are shown in panel (c), while in panel (e) the contours are for the magnetic field intensity in MG. Panel (b) is a zoom over the conical shock region depicted in (c), and shows additionally the region where the flow is submagnetosonic, $M_{\rm ma} < 1$ (dashed line). Panel (d) is a cut perpendicular to the jet at $z = 17$ mm. Panel (f) shows the profiles on axis of density, $\rho \times 10^6$ (g cm^{-3}), axial velocity, v_z(km/s), and ion and electron temperatures (eV).

collimation of a (magnetically or thermally driven) wind is the consequence of the inertia of a dense, toruslike circumstellar envelope, which focuses the flow in the polar direction, forming prolate, wind-blown cavities, and jets [28–31]. Our results show for the first time that an axial magnetic field can in fact mimic the action of a structured, dense envelope, and that the complex physics of jet collimation can be directly accessed in the laboratory.

Finally, the third phase corresponds to the propagation of the jet, which undergoes one or more expansions and compressions that may also lead to the further generation of shocks (interesting similarities exist with jets in ultrafast accelerative flames in obstructed channels [32]). An example of such a refocusing event can be seen in Fig. 2(e), where the contour lines tracing the magnitude of the magnetic field show a new region of compression at the tip of the jet ($z \sim 23$ mm). Figure 2(f), which illustrates the plasma properties in the jet, shows the profiles on axis, at 26 ns, of the axial velocity, electron and ion temperatures, and mass density. The shock-heated jet has relatively low densities, and thermal equilibration between the ions and electrons is slow, leading to decoupled temperature. The jet emerging from the conical shock is aligned with the magnetic field and it is potentially susceptible to firehose instability, which may disrupt the flow through long (axial) wavelength, helical-like distortions (e.g., Ref. [33]). The condition of growth requires anisotropic pressures, $P_\parallel - P_\perp > B^2/4\pi$, where the parallel $P_\parallel$ and perpendicular $P_\perp$ pressures generally include both the thermal pressure, and the ram pressure due to the bulk motion of the flow (ρv^2). For the highly supersonic, field-aligned flows of interest here, the parallel pressure is $P_\parallel \sim \rho v^2$, and the stability condition, assuming an isotropic thermal pressure, reduces to $M_A^2 - \beta/3 > 1$, where M_A is the Alfvenic Mach number, and β is the ratio of thermal to magnetic pressure. Although this is only marginally met in the jet's core, the presence of a dense, strongly magnetized plasma at larger radii, may provide the apparent stabilization of the flow [33]. Figure 3 shows a three-dimensional view of the flow at 25 ns. The axial structure consists of alternating regions where the radius of the flow, $r_f(z)$, and curvature of the magnetic field lines change from convex to concave. In the regions where the plasma is radially bulging out, a Rayleigh-Taylor type filamentation instability can develop, with the conditions for its growth being similar to those of a theta pinch [34,35]. In particular, the growth rate, Γ, for

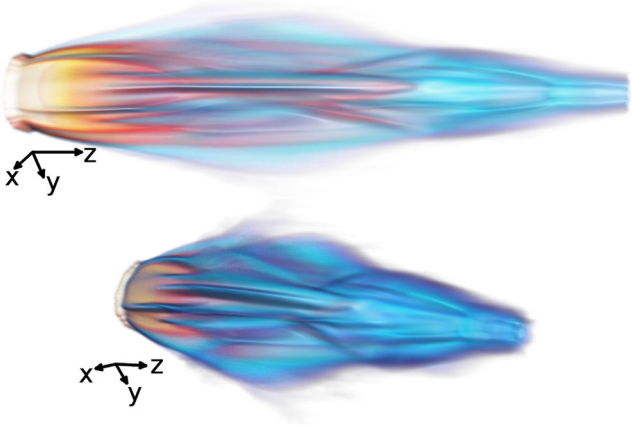

FIG. 3 (color online). Volume rendering of density at 25 ns, showing the structuring of the flow by the RT filamentation instability.

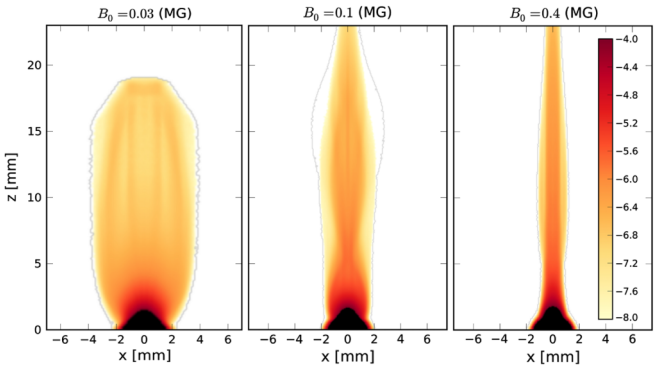

FIG. 4 (color online). Line-of-sight integrated density, ($\int \rho dy$) in g cm^{-2} on a logarithmic scale, at $t = 30$ ns, for an Al target and laser intensity $I = 1.5 \times 10^{13}$ W cm^{-2}.

large azimuthal mode numbers m, with wave number $k_\theta = m/r_f$, is given by the classical result $\Gamma \sim \sqrt{gk_\theta}$, where g is the effective gravity at the plasma-vacuum interface, which can be approximated as $g \sim c_A^2/R_c$, where R_c is the radius of curvature [35]. In addition, as the flow streams along the curved walls of the cavity with a velocity $v \gtrsim c_A$, it experiences an additional centrifugal acceleration of the same order of magnitude. Making the simplifications $R_c \sim R_{\rm coll}$ and $v \sim v_{\rm exp}$, which are valid at early times, shows that the characteristic growth time scale of the instability is short, of the order of the collimation time scale, $\tau_I \sim \tau_{\rm coll}/\sqrt{m}$. These estimates are consistent with the numerical results, which show azimuthal perturbations, $m \sim$ 8–16, growing within a few nanoseconds, and leading to the rapid filamentation of the outer edges of the cavity first, and of the jet beam later [see Figs. 2(d) and 3]. The radially growing perturbations also propagate axially with the flow [cf. Fig. 2(c)], and produce a relatively low density, broad halo surrounding the central core of the flow.

So far we have discussed the case of a relatively strong magnetic field, one that is able to generate jets via a conical shock. For weaker fields in contrast, the flow streamlines tend to become parallel to the magnetic field lines, and the flow remains instead collimated in a cylindrical cavity, without jets. The effects that changing the applied magnetic field has on the collimation and morphology of the flow is elucidated in Fig. 4, which shows for a fixed laser intensity the line-of-sight, integrated mass density. Indeed the flow structure changes from a cylindrical cavity ($B_0 \lesssim$ 0.03 MG), delineated by a denser shell of plasma, to a prolate cavity with a jet emerging from a focusing, conical shock. For the largest field values ($B_0 \gtrsim 0.2$ MG), the focusing conical shock is closer to the target, and the result is a denser and narrower jet, which is relatively homogeneous. We note that placing a massive target in the jet propagation path would lead to the formation of a reverse shock in the jet, in a configuration ideal to studying accretion shocks and magnetized accretion columns in young stars [36]. Finally, we find that although different target materials lead to qualitatively similar results, increasing the atomic number of the target, and thus the radiative losses from the plasma, tends to produce better collimated jets. This is a well-known result from nonmagnetized jet experiments [14].

The astrophysical relevance of laboratory flows rests on their dynamics being well approximated by ideal magnetohydrodynamics [7], which implies the advective transport of momentum, magnetic field, and thermal energy, to dominate over diffusive transport. In this regime the dimensionless Reynolds (Re), magnetic Reynolds (Re$_M$), and Peclet (Pe) numbers are much larger than unity. The simulations show that the bulk of the flow is well approximated as an ideal magnetofluid (Re $\sim 10^4$–10^5; Re$_M \sim 100$; Pe $\sim$ 10–20). Thus we expect astrophysical simulations of related flows, performed under equivalent, scaled initial condition to produce qualitatively similar results. From an astrophysical perspective, the results demonstrate that an axial magnetic field can on its own play the same role as a circumstellar envelope, and lead to flows similar to shock focusing models. Therefore providing an alternative route to explain the presence of jets when massive, collimating envelopes are not consistent with observations [37]. Moreover, the results suggest a new framework that combines the magnetic collimation of wide-angle flows with the generation of hydrodynamic jets, which do not suffer from potentially disruptive instabilities linked to the presence of a strong B_θ. The predicted formation of a standing conical shock is also compelling, as it could possibly explain the presence of stationary emission features observed close to young stellar jet sources [38,39]. Although the strength and topology of magnetic fields in those astrophysical jet sources remain a major open question [40], estimates of its intensity [41] ($\sim$10 mG) are consistent with those needed for collimation by a poloidal magnetic field.

The authors acknowledge the support from the Ile-de-France Grant No. E1127 and from the ANR "Blanc" Grant SILAMPA.

[1] R. E. Pudritz, M. J. Hardcastle, and D. C. Gabuzda, arXiv:1205.2073.

[2] R. D. Blandford and D. G. Payne, Mon. Not. R. Astron. Soc. **199**, 883 (1982).

[3] T. Matsakos, S. Massaglia, E. Trussoni, K. Tsinganos, N. Vlahakis, C. Sauty, and A. Mignone, Astron. Astrophys. **502**, 217 (2009).

[4] S. C. Hsu and P. M. Bellan, Phys. Rev. Lett. **90**, 215002 (2003).

[5] S. V. Lebedev, A. Ciardi, D. J. Ampleford, S. N. Bland, S. C. Bott, J. P. Chittenden, G. N. Hall, J. Rapley, C. A. Jennings, A. Frank, E. G. Blackman, and T. Lery, Mon. Not. R. Astron. Soc. **361**, 97 (2005).

[6] A. Ciardi, S. V. Lebedev, A. Frank, F. Suzuki-Vidal, G. N. Hall, S. N. Bland, A. Harvey-Thompson, E. G. Blackman, and M. Camenzind, Astrophys. J. Lett. **691**, L147 (2009).

[7] D. D. Ryutov, R. P. Drake, and B. A. Remington, Astrophys. J. Suppl. Ser. **127**, 465 (2000).

[8] J. P. Freidberg, Rev. Mod. Phys. **54**, 801 (1982).

[9] M. M. Romanova, G. V. Ustyugova, A. V. Koldoba, and R. V. E. Lovelace, Mon. Not. R. Astron. Soc. **399**, 1802 (2009).

[10] S. Matt, R. Winglee, and K.-H. Bhm, Mon. Not. R. Astron. Soc. **345**, 660 (2003).

[11] H. C. Spruit, T. Foglizzo, and R. Stehle, Mon. Not. R. Astron. Soc. **288**, 333 (1997).

[12] A. Ciardi and P. Hennebelle, Mon. Not. R. Astron. Soc. **409**, L39 (2010).

[13] B. A. Remington, R. P. Drake, and D. D. Ryutov, Rev. Mod. Phys. **78**, 755 (2006).

[14] D. R. Farley, K. G. Estabrook, S. G. Glendinning, S. H. Glenzer, B. A. Remington, K. Shigemori, J. M. Stone, R. J. Wallace, G. B. Zimmerman, and J. A. Harte, Phys. Rev. Lett. **83**, 1982 (1999).

[15] B. Loupias, M. Koenig, E. Falize, S. Bouquet, N. Ozaki, A. Benuzzi-Mounaix, T. Vinci, C. Michaut, M. Rabec Le Goahec, W. Nazarov, C. Courtois, Y. Aglitskiy, A. Ya. Faenov, and T. Pikuz, Phys. Rev. Lett. **99**, 265001 (2007).

[16] B. Albertazzi *et al.*, Rev. Sci. Instrum. (to be published).

[17] B. Meyer and G. Thiell, Phys. Fluids **27**, 302 (1984).

[18] M. Tabak, J. Hammer, M. E. Glinsky, W. L. Kruer, S. C. Wilks, J. Woodworth, E. M. Campbell, M. D. Perry, and R. J. Mason, Phys. Plasmas **1**, 1626 (1994).

[19] J. A. Stamper, K. Papadopoulos, R. N. Sudan, S. O. Dean, E. A. McLean, and J. M. Dawson, Phys. Rev. Lett. **26**, 1012 (1971).

[20] C. K. Li, F. H. Séguin, J. A. Frenje, J. R. Rygg, R. D. Petrasso, R. P. J. Town, P. A. Amendt, S. P. Hatchett, O. L. Landen, A. J. MacKinnon *et al.*, Phys. Rev. Lett. **99**, 015001 (2007).

[21] C. A. Cecchetti *et al.*, Phys. Plasmas **16**, 043102 (2009).

[22] S. Atzeni, A. Schiavi, F. Califano, F. Cattani, F. Cornolti, D. Del Sarto, T. V. Liseykina, A. Macchi, and F. Pegoraro, Comput. Phys. Commun. **169**, 153 (2005).

[23] S. P. Lyon and J. D. Johnson, LANL Technical Report No. LA-UR-92-3407, 1992.

[24] J. P. Chittenden, S. V. Lebedev, C. A. Jennings, S. N. Bland, and A. Ciardi, Plasma Phys. Controlled Fusion **46**, B457 (2004).

[25] A. Ciardi, S. V. Lebedev, A. Frank, E. G. Blackman, J. P. Chittenden, C. J. Jennings, D. J. Ampleford, S. N. Bland, S. C. Bott, J. Rapley, G. N. Hall, F. A. Suzuki-Vidal, A. Marocchino, T. Lery, and C. Stehle, Phys. Plasmas **14**, 056501 (2007).

[26] H. Hornung, Annu. Rev. Fluid Mech. **18**, 33 (1986).

[27] B. Balick and A. Frank, Annu. Rev. Astron. Astrophys. **40**, 439 (2002).

[28] J. Canto, Astron. Astrophys. **86**, 327 (1980).

[29] A. Frank and G. Mellema, Astrophys. J. **472**, 684 (1996).

[30] C.-F. Lee, M.-C. Hsu, and R. Sahai, Astrophys. J. **696**, 1630 (2009).

[31] M. Huarte-Espinosa, A. Frank, B. Balick, E. G. Blackman, O. De Marco, J. H. Kastner, and R. Sahai, Mon. Not. R. Astron. Soc. **424**, 2055 (2012).

[32] V. Bychkov, D. Valiev, and L.-E. Eriksson, Phys. Rev. Lett. **101**, 164501 (2008).

[33] G. Benford, Astrophys. J. **247**, 792 (1981).

[34] A. I. Kleev and A. L. Velikovich, Plasma Phys. Controlled Fusion **32**, 763 (1990).

[35] F. A. Haas and J. A. Wesson, Phys. Fluids **10**, 2245 (1967).

[36] S. Orlando, G. G. Sacco, C. Argiroffi, F. Reale, G. Peres, and A. Maggio, Astron. Astrophys. **510**, A71 (2010).

[37] S. Cabrit, C. Codella, F. Gueth, B. Nisini, A. Gusdorf, C. Dougados, and F. Bacciotti, Astron. Astrophys. **468**, L29 (2007).

[38] P. Hartigan and J. Morse, Astrophys. J. **660**, 426 (2007).

[39] P. C. Schneider, H. M. Günther, and J. H. M. M. Schmitt, Astron. Astrophys. **530**, A123 (2011).

[40] P. Hartigan, A. Frank, P. Varnire, and E. G. Blackman, Astrophys. J. **661**, 910 (2007).

[41] R. Bonito, S. Orlando, M. Miceli, G. Peres, G. Micela, and F. Favata, Astrophys. J. **737**, 54 (2011).